

# Analysis of KaiA–KaiC protein interactions in the cyano-bacterial circadian clock using hybrid structural methods

Rekha Pattanayek<sup>1</sup>, Dewight R Williams<sup>2</sup>,  
Sabuj Pattanayek<sup>1</sup>, Yao Xu<sup>3</sup>, Tetsuya  
Mori<sup>3</sup>, Carl H Johnson<sup>3</sup>, Phoebe L Stewart<sup>2</sup>  
and Martin Egli<sup>1,\*</sup>

<sup>1</sup>Department of Biochemistry, School of Medicine, Vanderbilt University, Nashville, TN, USA, <sup>2</sup>Department of Molecular Physiology and Biophysics, School of Medicine, Vanderbilt University, Nashville, TN, USA and <sup>3</sup>Department of Biological Sciences, Vanderbilt University, Nashville, TN, USA

The cyanobacterial circadian clock can be reconstituted *in vitro* by mixing recombinant KaiA, KaiB and KaiC proteins with ATP, producing KaiC phosphorylation and dephosphorylation cycles that have a regular rhythm with a ca. 24-h period and are temperature-compensated. KaiA and KaiB are modulators of KaiC phosphorylation, whereby KaiB antagonizes KaiA's action. Here, we present a complete crystallographic model of the *Synechococcus elongatus* KaiC hexamer that includes previously unresolved portions of the C-terminal regions, and a negative-stain electron microscopy study of *S. elongatus* and *Thermosynechococcus elongatus* BP-1 KaiA–KaiC complexes. Site-directed mutagenesis in combination with EM reveals that KaiA binds exclusively to the CII half of the KaiC hexamer. The EM-based model of the KaiA–KaiC complex reveals protein–protein interactions at two sites: the known interaction of the flexible C-terminal KaiC peptide with KaiA, and a second postulated interaction between the apical region of KaiA and the ATP binding cleft on KaiC. This model brings KaiA mutation sites that alter clock period or abolish rhythmicity into contact with KaiC and suggests how KaiA might regulate KaiC phosphorylation.

The EMBO Journal (2006) 25, 2017–2028. doi:10.1038/sj.emboj.7601086; Published online 20 April 2006

Subject Categories: structural biology

Keywords: cyanobacteria; electron microscopy; molecular clock; protein–protein interactions; phosphorylation

## Introduction

Circadian clocks are endogenous biological timers that rhythmically regulate numerous processes with an approximately 24-h period (Dunlap *et al.*, 2004). They exist in diverse

organisms, but cyanobacteria are the simplest organisms known to possess a clock (Johnson, 2004). In the model organism *Synechococcus elongatus* PCC 7942, the *kai* locus encodes three proteins, KaiA, KaiB and KaiC that are essential for proper circadian function (Ishiura *et al.*, 1998). The observation that Kai proteins (KaiA and KaiC) appear to positively and negatively regulate *kaiBC* transcription (Ishiura *et al.*, 1998) seemed to render the cyanobacterial clock consistent with a transcription/translation oscillatory (TTO) feedback model, believed to be at the core of all self-sustained circadian timers (Dunlap *et al.*, 2004). However, Kondo, Iwasaki and co-workers recently reported robust circadian rhythms under constant dark conditions or in the presence of transcription or translation inhibitors (Tomita *et al.*, 2005). The phosphorylation status of KaiC exhibited a circadian rhythm for more than 2 days despite the absence of *kaiABC* mRNAs or rhythmic Kai protein abundance. Clearly, the cyanobacterial circadian clock is able to function without *de novo* synthesis of clock gene mRNAs and the clock proteins, and the period is accurately determined without TTO feedback. Thus, KaiA, KaiB and KaiC comprise a minimal timing system that is also temperature-compensated (Tomita *et al.*, 2005) (Figure 1A). In addition, it has been demonstrated that these three purified proteins form a temperature-compensated molecular oscillator *in vitro* that exhibits rhythmic phosphorylation and dephosphorylation of KaiC (Nakajima *et al.*, 2005). Therefore, the KaiABC system is a unique target for a biochemical and structural dissection of the molecular basis of a biological clockwork.

Several breakthroughs have recently also been reported in the structural area. High-resolution structural information for all Kai proteins emerged in 2004 (Johnson and Egli, 2004; Golden, 2004). The crystal structure of full-length *S. elongatus* KaiA revealed a domain-swapped arrangement with three different dimer interfaces (Ye *et al.*, 2004). The structures of the C-terminal dimerization and KaiC-interacting domain of KaiA from *Thermosynechococcus elongatus* BP-1 were solved separately by X-ray crystallography (Uzumaki *et al.*, 2004) and NMR (Vakonakis *et al.*, 2004). The crystal structure along with data regarding mutant proteins implicated grooves above the dimerization interface on opposite faces of the dimer as potential sites for interaction with KaiC. A further crystal structure of KaiA and a structure of KaiB from *Anabaena* sp. PCC7120 revealed a thioredoxin-like fold for the latter (Garces *et al.*, 2004). A recent crystal structure of KaiB from *Synechocystis* PCC6803 showed formation of a tetramer with a positively charged perimeter, a negatively charged center and a zipper of aromatic rings important for oligomerization (Hitomi *et al.*, 2005). The authors also demonstrated the importance of the tetrameric state of KaiB for proper clock function using mutational data. We determined the crystal structure of the full-length KaiC protein from *S. elongatus* (Pattanayek *et al.*, 2004). The structure of KaiC,

\*Corresponding author. Department of Biochemistry, School of Medicine, Vanderbilt University, 607 Light Hall, Nashville, TN 37232, USA. Tel.: +1 615 343 8070; Fax: +1 615 322 7122; E-mail: martin.egli@vanderbilt.edu

Received: 7 February 2006; accepted: 17 March 2006; published online: 20 April 2006

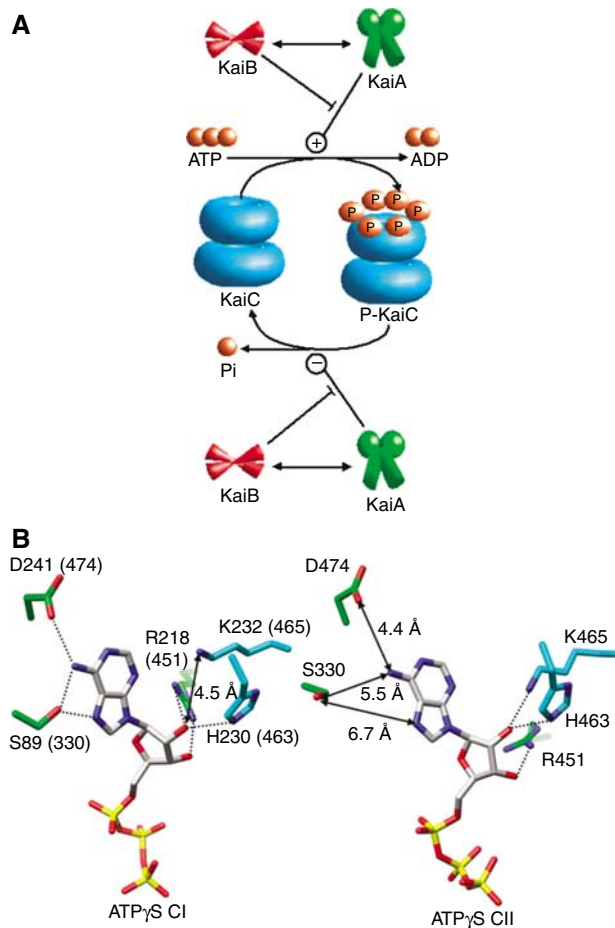


**Figure 1** Basic composition of the cyanobacterial circadian clock and ATP binding between subunits in the KaiCI and KaiCII halves. (A) The minimal cycle as established by Tomita *et al* (2005) and Nakajima *et al* (2005). The KaiA dimer is green, the KaiB tetramer is red, the KaiC hexamer is cyan, and phosphates are orange. The effect of KaiA is to inhibit dephosphorylation or to stimulate phosphorylation of KaiC. KaiB antagonizes the effect of KaiA (Iwasaki *et al*, 2002; Williams *et al*, 2002; Xu *et al*, 2003; Kitayama *et al*, 2003). (B) ATP binding sites in the KaiCI (left) and KaiCII halves (right). Carbon atoms of side chains from residues in adjacent subunits are colored in green and cyan. Hydrogen bonds ( $<3.2 \text{ \AA}$ ) are represented by dashed lines and selected distances are highlighted by solid arrows. The left panel indicates the CI residue and the corresponding CII residue is in parentheses.

the central and largest protein from the cyanobacterial clockwork, revealed the formation of a homo-hexamer in the shape of a ‘double-doughnut’ with a central pore and 12 ATP molecules bound between the interfaces of monomers. Interestingly, specific recognition of the nucleobase of ATP exists only in the N-terminal KaiCI half (Figure 1B). The structure also allowed the identification of three phosphorylation sites in the KaiCII domain (T426/S431/T432). However, KaiCI does not seem to contain any phosphorylation sites (Nishiwaki *et al*, 2004; Xu *et al*, 2004). These three residues, when mutated to alanine individually, destroy the rhythm *in vivo* and the triple mutant is no longer phosphorylatable. The C-terminal 22 residues of KaiC monomers were partly disordered in the crystal structure, suggesting high conformational flexibility in this region for the unbound state of KaiC. Vakonakis and LiWang (2004) recently reported

the NMR solution structure of a complex between the dimeric C-terminal KaiA domain and a 30-mer peptide derived from the C-terminus of KaiC for the cyanobacterium *T. elongatus* BP-1.

Although the combined structural data mark the beginning of an improved understanding of the mechanism of the KaiABC clockwork, no consistent model of the interactions between Kai proteins has been proposed thus far. Moreover, no experimental model for the KaiA–KaiC interaction has been reported, which sheds light on the regulation of KaiC phosphorylation by KaiA. Here, we present an improved crystallographic model, including the C-terminal flexible region, of the KaiC hexamer from *S. elongatus*. The structures we observe for the C-terminal regions are likely to represent a subset of the possible conformations in solution. We also present a single particle reconstruction of the negatively-stained *T. elongatus* BP-1 KaiA–KaiC complex, as well as *in vitro* studies of complex formation between wild-type and mutant KaiC and KaiA proteins, and *in vivo* activity data for mutant KaiC proteins. The predominant KaiA–KaiC complex has a stoichiometry of one KaiA dimer to one KaiC hexamer, which we refer to as 1:1 stoichiometry. Analysis of the new structural and functional data indicates that KaiA binds to KaiC at the C-terminus of KaiC and that the KaiA dimer becomes tethered via a flexible linker region to the KaiC hexameric barrel. The flexible tethering raises the possibility that a second more transitory interaction might occur between additional surfaces of KaiA and KaiC. We present a model for the KaiA–KaiC complex with a second interaction site between KaiA and KaiC that is consistent with all of the structural information of the component proteins, and which demonstrates that residues in KaiA whose mutation alters clock period or abolishes rhythmicity can be at least transiently near the KaiCII ATP binding region. This model for the KaiA–KaiC complex provides a satisfactory explanation for how a single KaiA dimer is able to interact with the KaiC hexamer and enhance the latter’s autokinase activity.

## Results and discussion

### Complete crystallographic model of *S. elongatus* KaiC

In the crystal structure of the KaiC homo-hexamer from *S. elongatus* determined to  $2.8 \text{ \AA}$  resolution (PDB-ID 1TF7), only residues E14 to I497 from the six chains (termed A–F) were incorporated (Pattanayek *et al*, 2004). Despite the presence of electron density above the C-terminal KaiCII dome, we initially refrained from attempting to build the missing C-terminal residues of individual chains (T498 to S519) due to the poor quality of the electron density in this region. The recently reported NMR model of two C-terminal peptides from *T. elongatus* BP-1 KaiC (*ThKaiC*; residues G488 to E518) bound to the dimer formed by C-terminal domains of *ThKaiA* (Vakonakis and LiWang, 2004) prompted us to revisit the C-terminal region in the crystal structure of the KaiC hexamer.

Careful inspection of the electron density map and monitoring of the extensions of C-terminal regions with the help of a series of omit maps allowed us to fully complete chains A and F (Figure 2A). Conjugate-gradient minimizations were performed each time a questionable portion of the model was deleted to reduce bias. An example of an omit map around residues 509–511 of the F chain is shown in Figure 2B. Chain

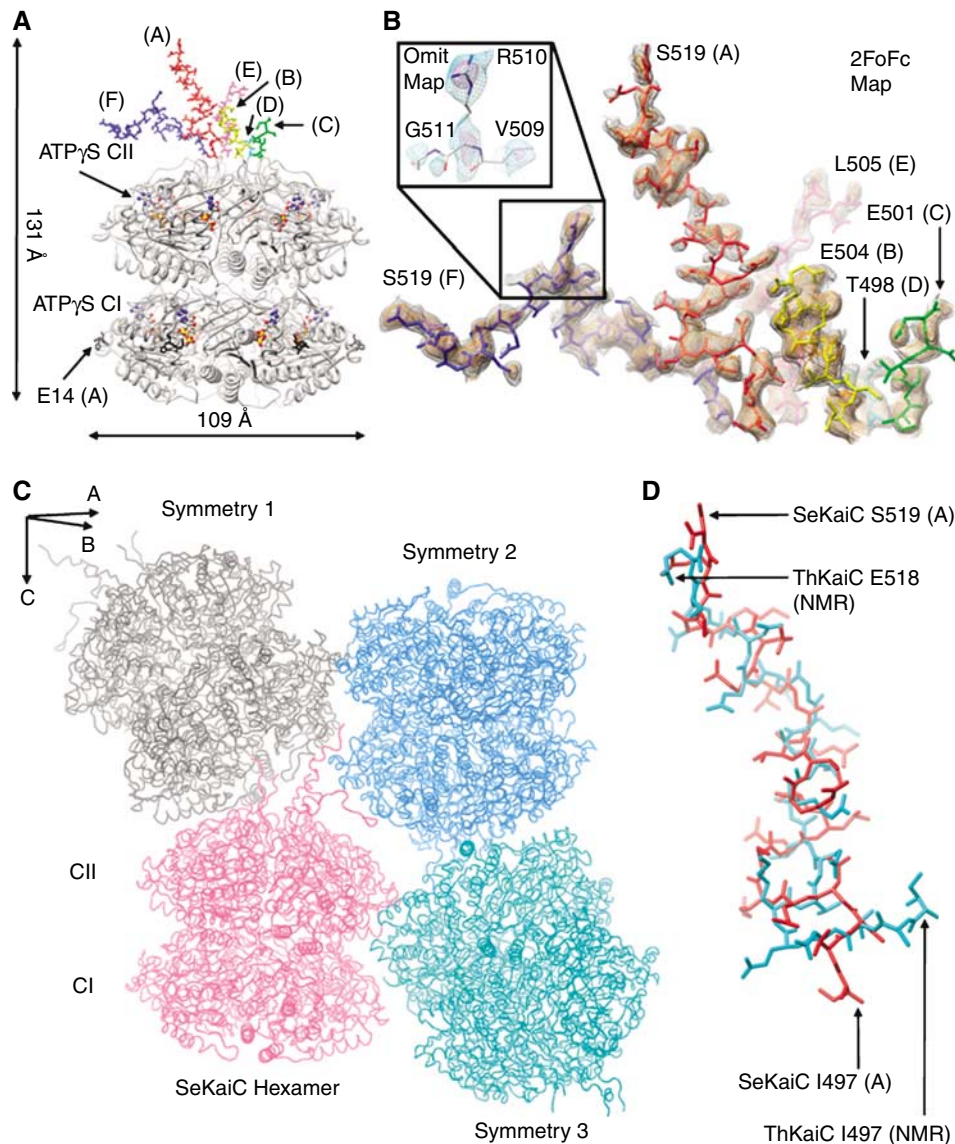


**Figure 2** Complete crystallographic model of *S. elongatus* KaiC including the C-terminal region. **(A)** Structure of *S. elongatus* KaiC with the C-terminal region partly resolved. The CI and CII halves are displayed as gray ribbons. The partially completed A, B, C, D, E, and F C-terminal peptides are labeled. N-terminal residues 14 and 15 are in black and are shown as sticks. The ATP $\gamma$ S molecules bound between subunits in CI and CII are shown in van der Waals mode and the color code for atoms is the same as in Figure 1B. **(B)** Quality of the final Fourier sum ( $2F_o - F_c$ ) electron density around the C-terminal peptide region (gray  $0.7\sigma$  and orange  $1.0\sigma$  level). Peptide chains A–F are colored as in Figure 2A. Top left: Omit map in the region marked by the black box (cyan  $0.7\sigma$  and magenta  $1.0\sigma$  level). **(C)** Packing interactions in space group  $P2_12_12_1$ ; four symmetry-related KaiC hexamers are colored in magenta, gray, cyan and green. **(D)** Structural comparison between the NMR *ThKaiC* C-terminal domains and the crystallographic model of the C-terminal end of the *SeKaiC* A-chain: r.m.s. deviation 2.1 Å. NMR peptide residues I497–E518 (413–434 C-chain in PDB-ID 1SU9) are shown in cyan and crystallographic A-chain peptide residues I497–S519 are shown in red. The corresponding r.m.s.d. for F-chain atoms amounts to 3.2 Å.

B of the starting model was extended by seven residues, four residues were added to chain C, one was added to chain D, and eight to chain E (Figure 2A and B). A summary of selected crystal data and refinement parameters for the new model is provided in Supplementary Table S1 (Supplementary data). The higher average B-factor for atoms in the C-termini ( $91 \text{ \AA}^2$ ) compared to the rest of the hexamer ( $74 \text{ \AA}^2$ ) provides an indication of the increased flexibility in this region.

Residues N485 to I497 form an S-shaped loop in each of the six subunits that make up the funnel-like opening of the channel on the KaiCII side. Arginines 488 protrude into the channel and partially seal it about 10 Å below the dome-

shaped surface of KaiCII (see Figure 1; Pattanayek *et al*, 2004). After residue T495, the chains project away from the surface of the KaiCII domain and the six-fold non-crystallographic symmetry that relates subunits inside the CI and CII halves breaks down. The conformations of C-terminal ends of chains A and F differ considerably. The former protrudes nearly vertically from the KaiCII dome surface (Figure 2A and B). The F chain follows the direction of chain A up to residue 502, but then assumes a sharp turn and the S503–S519 peptide runs approximately perpendicular to the six-fold axis of the KaiC complex.

The conformation of the KaiCII-terminal tails in the crystal structure is undoubtedly affected by packing interactions

between hexamers. In the orthorhombic lattice (space group  $P2_12_12_1$ ), the molecular six-fold rotation axes of individual molecules are tilted by ca.  $30^\circ$  relative to the crystallographic  $c$ -direction (Figure 2C). Molecules are arranged head-to-tail and the CII dome region is positioned near the central channel at the N-terminal KaiCI region of another hexamer, which exhibits a strongly negative electrostatic surface potential (Pattanayek *et al*, 2004). It is likely that the degree of order of the C-terminal peptides is influenced by this electrostatic potential as well as by steric constraints. Interestingly, the conformation of the C-terminal region of the A-chain in the improved *SeKaiC* crystal structure resembles that of the *ThKaiC*-peptide bound to the C-terminal domain of *ThKaiA* in the NMR structure (Figure 2D).

The new model offers a more complete view of the topological and conformational properties of the KaiCII domain. The C-terminal peptides protrude from the CII dome in a tentacle-like fashion, potentially serving as handles for interactions with the two other Kai proteins, KaiA (Vakonakis and LiWang, 2004) and KaiB (to date there is no evidence for such a binding mode). Although *kaiC* is an internally duplicated version of a *recA/dnaB*-like gene (Iwasaki *et al*, 1999; Leipe *et al*, 2000), the structure now demonstrates that the C-terminal regions of the CI and CII halves have different conformations. The C-terminal regions of the CI half form the linkers between the CI and CII domains, while the C-terminal regions of the CII half protrude from the CII dome of the hexamer. The N-terminal 13 residues per subunit, currently not visible in the crystal structure, emerge from the side of the CI ring rather than from the CI channel opening (Figure 2A). Therefore, the CI and CII sides of the hexamer are distinct in that only the CII side has single-stranded peptide extensions protruding from the vicinity of the central channel.

### EM analysis of the KaiA–KaiC complex

The structural work performed thus far on KaiA, KaiB and KaiC has been on proteins from several different species of cyanobacteria, including *S. elongatus* (*Se*) and *T. elongatus* BP-1 (*Th*). The *SeKaiC* and *ThKaiC* proteins have homologous sequences (Figure 3), and thus are likely to have nearly identical structures. We attempted to isolate stable KaiA–KaiC complexes from both species for EM studies (Figure 4).

Full-length recombinant *SeKaiA* and *SeKaiC* proteins were prepared as described in Pattanayek *et al* (2004). However, native gel experiments did not show a well-resolved band for the *SeKaiA*–KaiC complex (Figure 4B). Since *SeKaiC* has to be purified in the presence of hydrolysable ATP in order to avoid precipitation, it is likely that the phosphorylation state of the recombinant *SeKaiC* hexamer, with three residues T426, S431 and T432 in the CII domain phosphorylated (Pattanayek *et al*, 2004; Xu *et al*, 2004), hampers the formation of a stable *SeKaiA*–KaiC complex *in vitro*.

In contrast, KaiC proteins from the thermophilic cyanobacteria *Synechococcus* sp. P2 (Mori *et al*, 2002) and *T. elongatus* BP-1 can be expressed and purified as monomers (Hayashi *et al*, 2003, 2004a). Thus, phosphorylation (with ATP) and hexamerization (with AMPPNP) can be performed separately, and this is advantageous for isolation of a stable KaiA–KaiC complex. Full-length recombinant *ThKaiA* and *ThKaiC* proteins with N-terminal (His)<sub>6</sub> tags were prepared and KaiC hexamer formation was induced with AMPPNP.

Complex formation was verified by native PAGE. Upper bands in lanes 3 and 4 of Figure 4A represent complex and middle and lower bands correspond to residual *ThKaiC* hexamer and *ThKaiA* dimer, respectively. Samples revealing the presence of a high molecular weight complex and relatively low amounts of free *ThKaiA* dimer and *ThKaiC* hexamer were used for negative-stain EM.

Several hundred micrographs were collected of negatively stained *ThKaiC*, *ThKaiA*–KaiC, *SeKaiC* and *SeKaiA*–KaiC samples. Approximately 4000 particle images were extracted for each sample and class sum images were generated to enhance the features of the particle images (Figure 5A). Both *ThKaiC* and *SeKaiC* class sum images appear similar to projections of the crystallographic structure of *SeKaiC* with six-fold ring-shaped top views and bell-shaped or four-lobed blossom-shaped side views. Roughly 30% of the *ThKaiA*–KaiC class sum images reveal a plume of additional density, assigned to KaiA, protruding from one end of the KaiC hexamer (Supplementary Figure S2, Supplementary data). A smaller percentage (<5%) of the *SeKaiA*–KaiC class sum images show weak but similar density protruding from the hexamer.

In order to visualize the location of KaiA within the complex in three dimensions, single particle reconstructions were calculated. *ThKaiC* and *SeKaiC* reconstructions resemble the crystallographic structure of *SeKaiC* filtered to moderate resolution (Figure 5B). Previous EM studies also produced a hexameric model or reconstruction of KaiC (Mori *et al*, 2002; Hayashi *et al*, 2003; Vakonakis *et al*, 2004). Unfortunately, reconstruction of the *SeKaiA*–KaiC particle images showed no density for KaiA, presumably due to the instability of the complex. However, a reconstruction of the *ThKaiA*–KaiC complex has additional density on one end protruding from a region near the central channel (Figure 5C). When the isosurface level is lowered, the *ThKaiA*–KaiC reconstruction shows two plumes of weak density extending in opposite directions. This indicates that KaiA is not bound in a defined orientation, but rather occupies a variety of positions relative to the KaiC hexameric barrel.

Close examination of class sum images of *ThKaiA*–KaiC with matching projections of the *ThKaiA*–KaiC reconstruction shows that the KaiA density is both blurred and weaker in projections of the reconstruction (Figure 5D). This is a second indication that KaiA is attached to the KaiC hexameric barrel by an extended and flexible peptide tether. Individual particle images of *ThKaiA*–KaiC filtered to 20 Å resolution show a dimeric structure that resembles the crystal structure of the KaiA dimer (Ye *et al*, 2004) (Figure 5E). The density assigned to the KaiA dimer is spaced from the hexameric barrel of KaiC by ~35 Å.

### A C-terminal deletion in KaiC prevents KaiA:KaiC complex formation and abolishes rhythmicity

The presence of single-stranded peptides known to bind KaiA protruding from the CII-end of KaiC and the absence thereof on the CI side suggests that the KaiA density observed in the *ThKaiA*–KaiC reconstruction is located on the CII half of KaiC. For verification, we generated a *ThKaiC* deletion mutant lacking the C-terminal 25 amino acids ( $\Delta 25CThKaiC$ ). Native PAGE indicates that the deletion does not affect hexamerization but prevents binding by *ThKaiA* (Figure 4C,

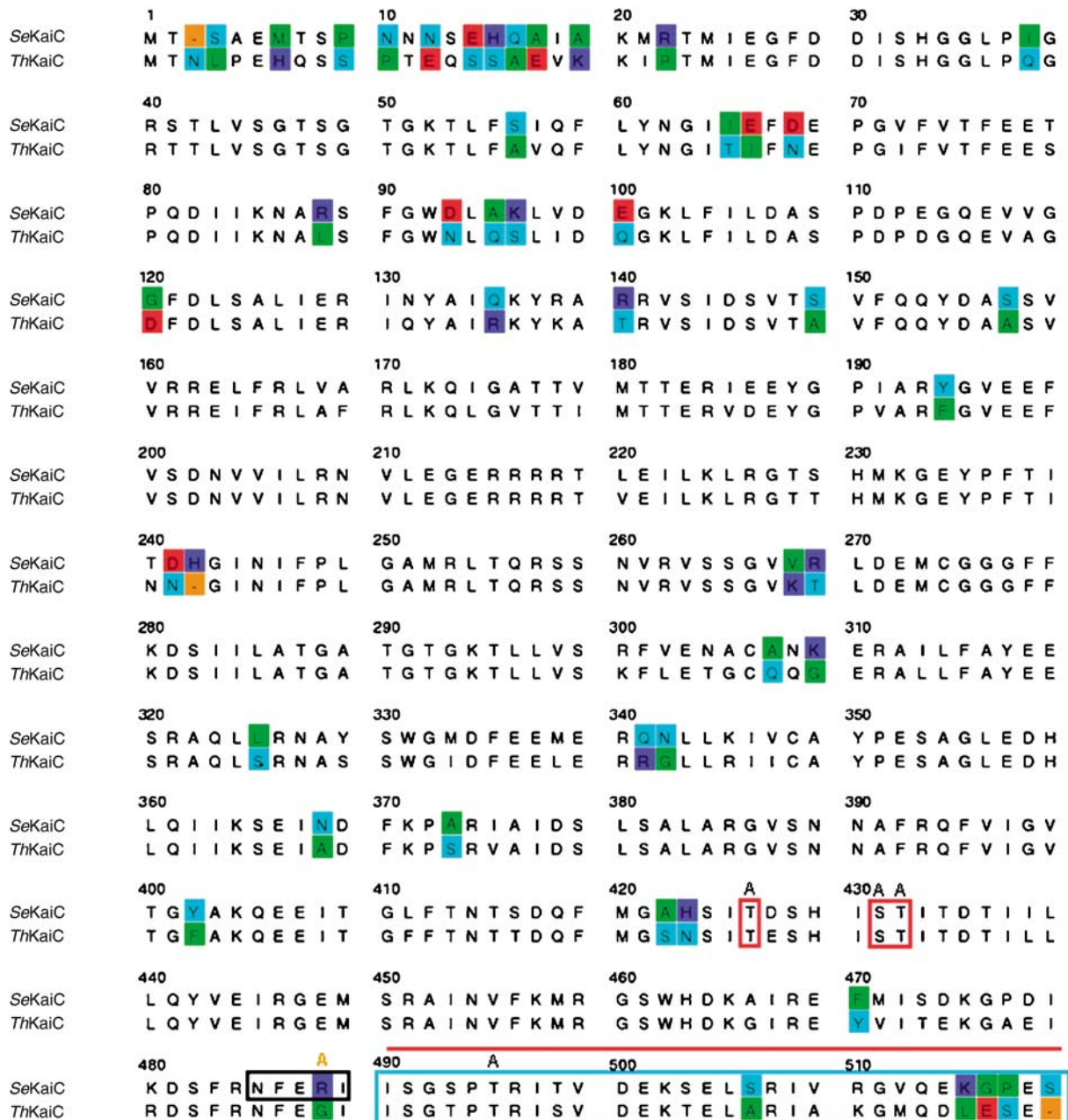


**Figure 3** Sequence alignment for the KaiC proteins from *S. elongatus* (SeKaiC) and *T. elongatus* (ThKaiC): 80% identity and 91% similarity. The numbering corresponds to SeKaiC. Gaps (i.e. '-' characters) are highlighted in orange. Dissimilar amino acids are highlighted: green for hydrophobic (A, F, G, I, L, M, P, V or W), cyan for hydrophilic (C, N, Q, S, T or Y), red for negatively charged (D or E), and blue for positively charged (H, K or R). Phosphorylation sites are indicated by red boxes, and mutation of these residues to alanine destroys rhythmicity *in vivo*. The SeKaiC R488A mutation is indicated above this sequence position in orange. Solid lines indicate residues deleted in this study (red: *in vivo* analysis; gold: native gels and EM). The cyan and gray boxes highlight residues of ThKaiCII studied in the NMR structure that were morphed into the SeKaiCII peptide in the complex models. Residues marked by the gray box form the short linker between the surface of KaiCII and the portion of the C-terminal CII peptide bound to KaiA in the engaged model (Figure 8B).

lanes 2 and 5, respectively). Negative-stain EM further corroborates this finding, as class sum images and a reconstruction of the ThKaiA and  $\Delta 25CThKaiC$  mixture show no evidence of complex formation (Figure 6; Supplementary Figure S2, Supplementary data).

We also assessed the consequences of a C-terminal deletion on circadian rhythms *in vivo*. Earlier work established that when the *kaiC* gene is deleted, cyanobacteria exhibit arrhythmic luminescence patterns (Ishiura *et al*, 1998).

However, when wild-type SeKaiC is expressed in a *kaiC* null strain of cyanobacteria under the control of an IPTG-derepressible promoter (*trcp*), rhythmicity is restored in a population of cells (Xu *et al*, 2003; Nakahira *et al*, 2004) (Figure 7A, left panel). As shown in Figure 7A (center panel), expression of *S. elongatus*  $\Delta 30CKaiC$  under regulation of *trcp* in the *kaiC*-null strain does not allow rhythmicity to be restored at various expression levels induced by IPTG. Conversely, *in vivo* testing of a SeKaiC R488A mutation reveals an unaltered

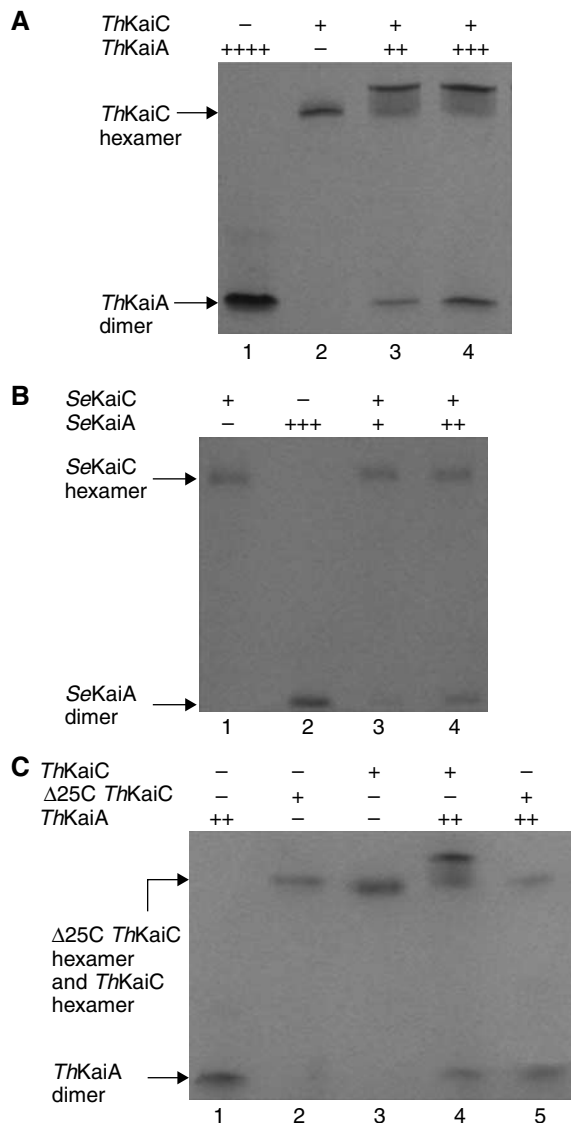


**Figure 4** Gel assays for KaiC hexamerization and KaiA–KaiC complex formation with wild type and a C-terminal deletion mutant of KaiC ( $\Delta 25CThKaiC$ ). (A) Native gel-electrophoretic assay for the formation of the complex between full-length *ThKaiA* dimer and *ThKaiC* hexamer. A ‘+’ indicates a 10 pM concentration of KaiA dimer and a 15 pM concentration of KaiC hexamer. Additional ‘+’ signs indicate increases by 10 and 15 pM in the concentrations of the KaiA dimers and KaiC hexamers, respectively. A ‘–’ indicates absence of protein. (B) Native gel-electrophoretic assay for the formation of the complex between full-length *SeKaiA* dimer and *SeKaiC* hexamer. See (A) for explanation regarding protein concentrations. (C) Native gel-electrophoretic assay showing absence of complex formation in mixtures of full-length *ThKaiA* dimer and  $\Delta 25CThKaiC$  hexamer. See (A) for explanation regarding protein concentrations.

period but a strongly damped oscillation (Figure 7A, right panel, 1  $\mu$ M IPTG). We were originally interested in residue R488 because arginines in an extended conformation from six subunits virtually seal the channel at the CII end in the crystal structure. As with wild-type *SeKaiC*, when the IPTG concentration is increased, the damping of the oscillation is strongly enhanced. Consistent with the data from native PAGE with  $\Delta 25CThKaiC$  (Figure 4C), a native-gel immunoblotting assay for wild-type *SeKaiC* and the  $\Delta 30CSeKaiC$  and *SeKaiC* R488A

mutants expressed in *kaiC*-null cyanobacterial strains demonstrates that neither the deletion nor the site-specific single mutation affect hexamerization of *SeKaiC* (Figure 7B).

Together, the EM results and *in vivo* circadian data provide unequivocal evidence that the KaiA-binding site on KaiC is restricted to the CII half. Removing the entire C-terminal peptide abolishes binding by KaiA and circadian rhythmicity. The R488A mutation seriously impairs proper function of KaiC *in vivo* and causes variability in the period lengths of cells within the population. Therefore, the observed oscillation damps as the cells become asynchronous with each other. An improved structural model is necessary to understand the effect of the R488A mutation on the KaiA–KaiC complex.

### Models of the KaiA–KaiC complex and implications for the action of KaiA on KaiC

NMR studies show that the KaiC C-terminal region binds in the groove formed between the C-terminal domains of the KaiA dimer (Vakonakis *et al*, 2004). The improved crystallographic model of *SeKaiC* indicates that the six potential KaiA-binding peptides in a KaiC hexamer have divergent structures that are presumably flexible in solution. Our EM results reveal that the binding of KaiA to KaiC results in a variable orientation of the KaiA dimer relative to the hexameric barrel of KaiC, consistent with the variable conformations of the six potential binding sites and the flexibility of the KaiC C-terminal peptides. However, this image of the KaiA–KaiC complex does not provide an explanation for enhancement of KaiC-phosphorylation by KaiA, or, alternatively, inhibition of dephosphorylation. We propose that the initial interaction between KaiA and the C-terminal peptides of KaiC serves to tether the KaiA dimer to the KaiC hexameric barrel, and that the flexibility of this connection leads to a second functionally important interaction between additional residues in KaiA and KaiC.

Guided by the *ThKaiA*–KaiC reconstruction (Figure 5C, bottom row), we built two models of the KaiA–KaiC complex that leave the binding interface identified by NMR between the KaiA dimer and the KaiC C-terminal peptide mostly intact (Vakonakis and LiWang, 2004). The relative orientation of the KaiA C-terminal and N-terminal domains observed in the crystal structure of full-length KaiA from *S. elongatus* is maintained in the models (the dimer interface III; Ye *et al*, 2004). The first model, which we refer to as the ‘tethered’ model, has KaiA positioned into one of the two plumes of KaiA density in the *ThKaiA*–KaiC reconstruction with KaiA  $\sim 35$  Å from the KaiC hexameric barrel (Figure 8A). In order to place KaiA in this position, we kept residues 501–518 of the NMR KaiC peptide fixed. Then we extended residues 485–500 of the peptide away from the KaiA C-terminal domain by altering the backbone torsion angles of residue 499. We also found the length of the original peptide (485–500) to be approximately equal to the distance between KaiA and KaiC in the *ThKaiA*–KaiC reconstruction ( $\sim 35$  Å). The second model, which we refer to as the ‘engaged’ model, also fits within the EM density and has the KaiA dimer in close proximity to the KaiC hexameric barrel (Figure 8B). To generate this model, we preserved the conformation of the NMR KaiC peptide (490–518) and changed the backbone torsion angles of residue 489 to form a short compact linker region from 485 to 489. Given the moderate resolution of the

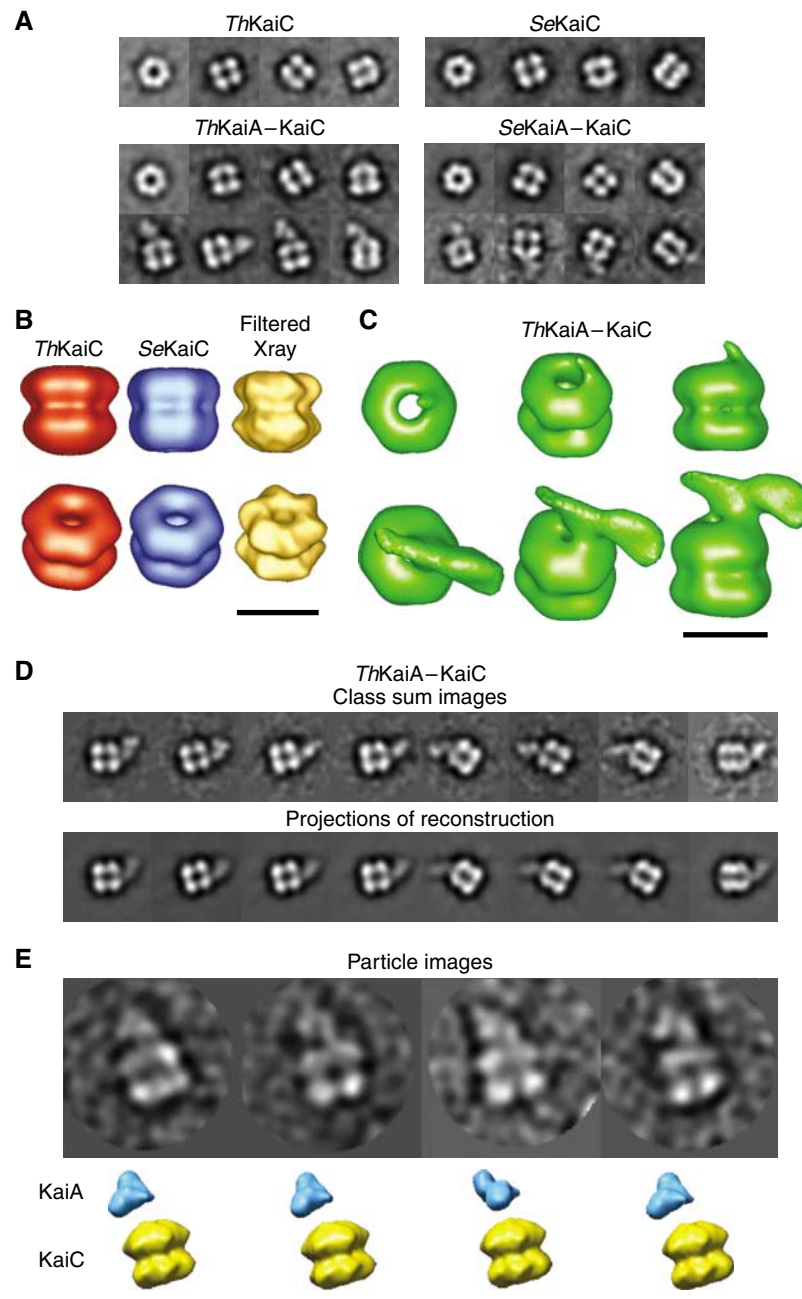


**Figure 5** Electron microscopy of KaiC and KaiA–KaiC complexes. (A) Selected class sum images of *ThKaiC*, *ThKaiA–KaiC*, *SeKaiC* and *SeKaiA–KaiC*. For each sample ~4000 particle images from negative-stain electron micrographs were averaged to generate 200 class sum images with improved signal-to-noise ratios over the input images. Class sum images representing top and side projection views are shown. Two rows of class sum images are shown for *ThKaiA–KaiC* and *SeKaiA–KaiC*, with the top row showing no discernible KaiA density and the bottom row showing a plume of KaiA density protruding from one end of the KaiC hexameric barrel. Approximately 30% of the *ThKaiA–KaiC* class sum images, and <5% of the *SeKaiA–KaiC* class sum images, show KaiA density. (B) Single particle reconstructions of *ThKaiC* (red) and *SeKaiC* (blue) at 24 Å resolution shown in two views (0° and 45°) compared to the crystal structure of KaiC (gold) filtered to 25 Å resolution. (C) Single particle reconstruction of *ThKaiA–KaiC* at 24 Å resolution shown in three views (90°, 45° and 0°) and with two isosurface values. Two plumes of weak, diffuse KaiA density, visible with the lower isosurface value connect to the KaiC hexameric barrel near the central channel. Small regions of disconnected density at the noise level were removed in the figures with the lower isosurface value (bottom row). (D) Matching pairs of *ThKaiA–KaiC* class sum images (top row) and projections of the *ThKaiA–KaiC* reconstruction (bottom row). (E) Individual particle images of *ThKaiA–KaiC* filtered to 20 Å resolution (top row) compared to 25 Å filtered representations of the KaiA (blue) and KaiC (gold) crystal structures. The scale bars represent 100 Å.

*ThKaiA–KaiC* reconstruction and the observation that KaiA is tethered to KaiC by a flexible linker, a more precise model of the complex cannot be built.

In both the tethered and engaged models, KaiC residue R488 is within the linker region (Figure 8) and mutation of

this residue to alanine seriously impairs proper function of the clock *in vivo* (Figure 7A). Conceivably, the R488A mutation in *SeKaiC* affects the degree of flexibility of the linker as well as electrostatic interactions in the region. It should be noted that the *ThKaiC* sequence has a glycine at this position

(Figure 3), which may be related to activity at high temperatures. Unlike the mutation of the conserved residue T495 to alanine that was previously shown to cause arrhythmicity (Ishiura *et al*, 1998; Taniguchi *et al*, 2001), R488A may be too far away from the KaiA dimerization interface to cause such a severe penalty on the period of the circadian clock.

KaiA dimerization involves domain swapping and the C-terminal domain of monomers consists of a four-helix bundle (see also Figure 1A in Ye *et al*, 2004). As can be seen in an

enlarged view of the engaged model, the apical portion of the bundle ( $\alpha$ 8-turn- $\alpha$ 9; nomenclature by Ye *et al*, 2004) from one KaiA monomer can come within  $\sim 12$  Å of the ATP binding site on the KaiC hexameric barrel (Figure 9). A host of mutations in the apical loop region of KaiA exhibit a short or long period phenotype (Ishiura *et al*, 1998; Nishimura *et al*, 2002; Uzumaki *et al*, 2004). Sequence alignment with KaiA's from various organisms shows that all of these residues (E239, M241, D242, E243, F244, A245, R249) are either conserved or chemically similar (Ye *et al*, 2004). In addition, the KaiA R249A mutation was found to significantly reduce the binding affinity between KaiA and KaiC (Garces *et al*, 2004). Mutation of KaiC residues either forming part of the ATP binding pocket or located on the surrounding area of the dome-shaped CII surface result in altered clock periods or cause arrhythmia (Ishiura *et al*, 1998; Taniguchi *et al*, 2001; Pattanayek *et al*, 2004). These findings suggest a possible interaction of the apical region of KaiA with the ATP binding region of KaiC, which we are proposing in the engaged model.

It had previously been suggested that the KaiA–KaiC binding interface is situated in the waist region of the KaiC double hexamer (Taniguchi *et al*, 2001; Vakonakis *et al*, 2004) and an alternative theoretical model envisioned the refolded KaiA dimer inserted into the central channel of KaiC (Wang, 2005). The EM and modeling results presented here are not consistent with these views. Our mutagenetic analysis and EM data together indicate that KaiA binds exclusively to the C-terminal peptides protruding from the CII half of the KaiC hexamer. This interaction may enable a secondary contact between KaiA and the KaiC subunit interface harboring ATP. Given the presumed flexibility of the linker region in KaiC, the model cannot disclose the detailed interactions between KaiA and KaiC at the ATP binding site. The contact surfaces between the two proteins might be slightly different than

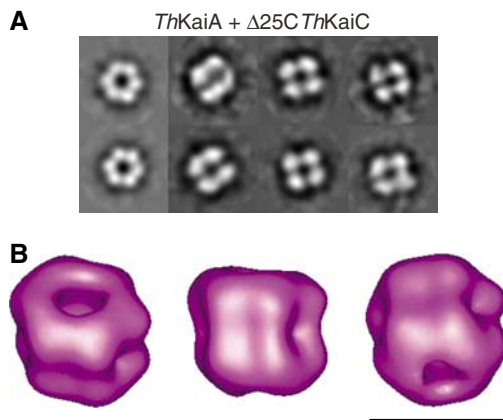


**Figure 6** Electron microscopy of a C-terminal deletion mutant of *ThKaiC* mixed with *ThKaiA*. (A) Selected class sum images of *ThKaiA* mixed with  $\Delta 25CThKaiC$ . Approximately 2600 particle images from negative-stain electron micrographs were averaged to generate 200 class sum images. Class sum images representing top and side projection views are shown. None of the 200 class sum images show density attributable to KaiA. (B) Single particle reconstruction of *ThKaiA* mixed with  $\Delta 25CThKaiC$  at 24 Å resolution shown in three views ( $-45^\circ$ ,  $0^\circ$  and  $45^\circ$ ). Note that no density is reconstructed for KaiA. The scale bar represents 100 Å.

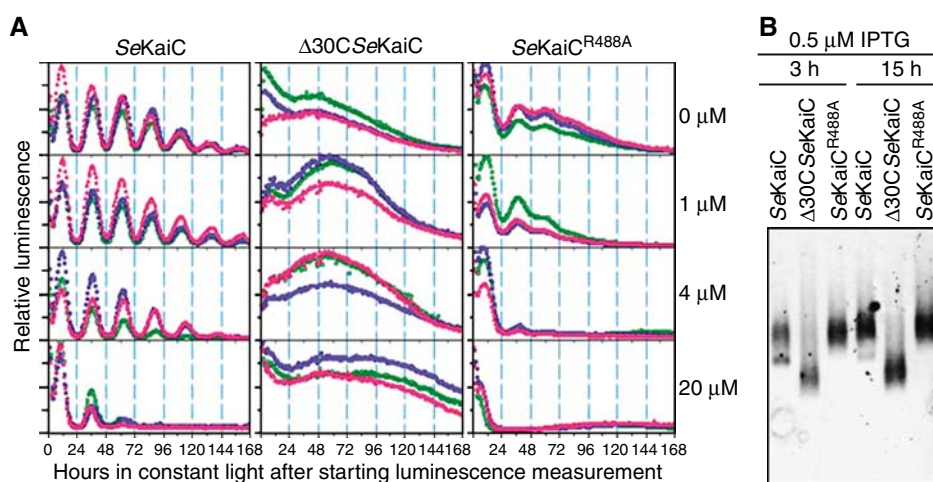


**Figure 7** Consequences of a C-terminal deletion in *S. elongatus* KaiC for clock function *in vivo*. (A) Deletion of the C-terminal 30 residues of *SeKaiC* abolishes circadian rhythmicity, and the R488A mutation attenuates rhythmicity. For regulation of expression levels of the *trcp*-driven wild-type *SeKaiC* (left) or mutant *SeKaiCs* [ $\Delta 30CSeKaiC$  (middle) and *SeKaiC*<sup>R488A</sup> (right)], after a 12 h dark pulse, 0, 1, 4 or 20  $\mu$ M of IPTG were applied at time 0 during the measurement of luminescence rhythms. Three representative luminescence traces are shown for each case. Overexpression of wild-type KaiC at high levels in *kaiC*-null strains can cause arrhythmicity (*SeKaiC*, panel A, bottom) as noted previously (Xu *et al*, 2003). (B) Native-immunoblotting assay for hexamerization of wild-type or mutant *SeKaiCs* ( $\Delta 30CSeKaiC$  and *SeKaiC*<sup>R488A</sup>). Cells were collected from the *kaiC*-null strains expressing *trcp::SeKaiC*, *trcp::Δ30CSeKaiC*, or *trcp::SeKaiC*<sup>R488A</sup> following 3 or 15 h of 0.5  $\mu$ M IPTG application at time 0. Total SDS-free extracts (2.5  $\mu$ g each) were resolved on a native gel in the presence of ATP, and then subjected to Western blot analysis of KaiC.

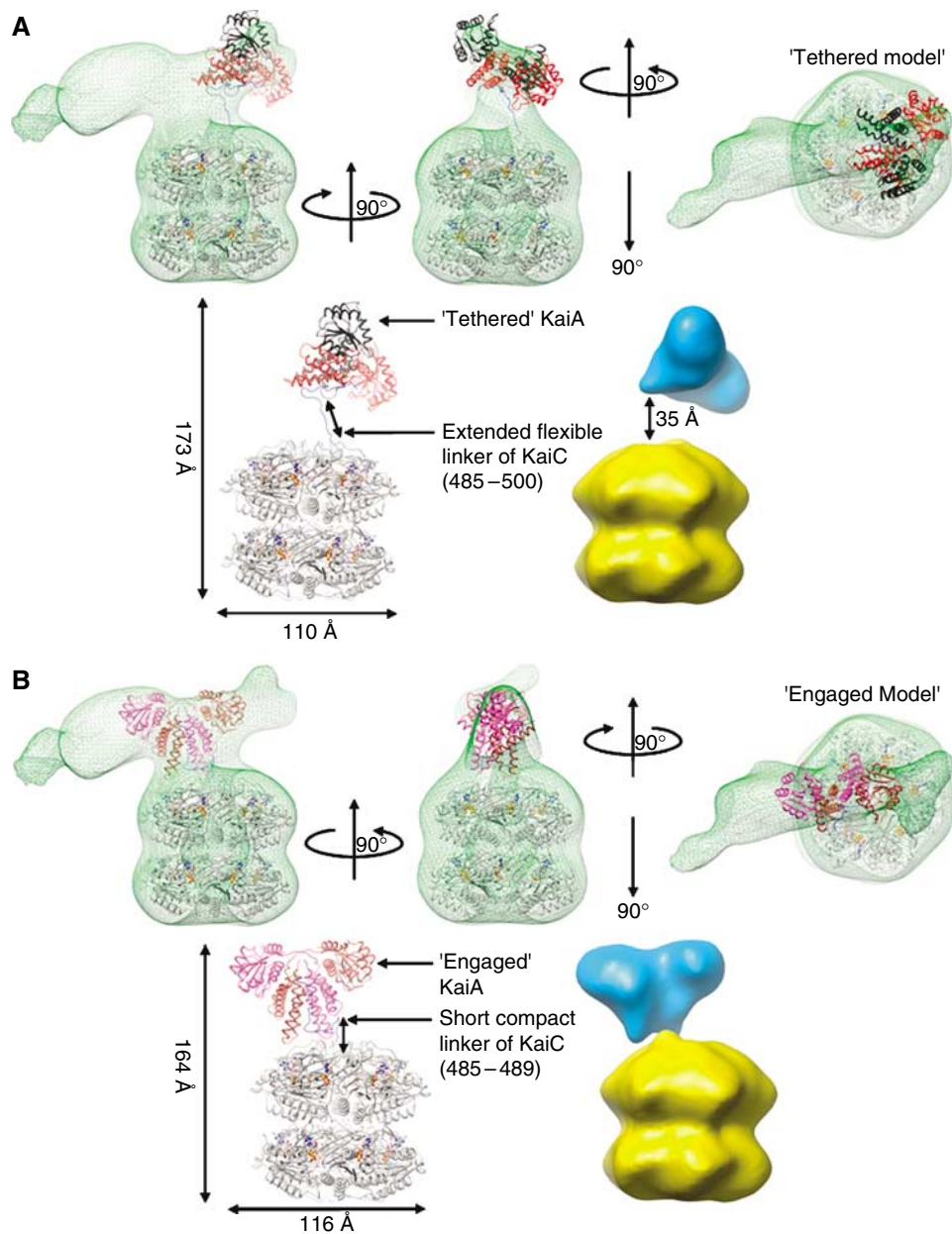


**Figure 8** EM-based models of the KaiA–KaiC 1:1 complex. **(A)** The ‘tethered model’ of the KaiA–KaiC complex. Three orientations are shown of ribbon representations of the KaiA dimer (red and black) and the KaiC hexameric barrel (colored as in Figure 2A) positioned within the EM reconstruction of *Th*KaiA–KaiC at a low isosurface value (green mesh). The proposed extended flexible linker region of KaiC (aa 485–500) is pointed out in the ribbon-only representation. The 35 Å gap between KaiA (blue) and the KaiC hexameric barrel (gold) is indicated in the 25 Å filtered density representation of the model. **(B)** The ‘engaged model’ of the KaiA–KaiC complex. Similar representation as in panel (A) for the ‘tethered’ model of the KaiA–KaiC complex but with the KaiA dimer shown in brown and magenta. The proposed short compact linker region of KaiC (aa 485–489) is pointed out in the ribbon-only representation.

depicted in the model. However, the proximity between a conserved surface of KaiA and the very center of the KaiC auto-kinase activity is intriguing. We showed previously that KaiC catalyzes the transfer of phosphate groups across subunits (Pattanayek *et al*, 2004; Xu *et al*, 2004). The enhancement may be related to a subtle conformational change on the surface that is transmitted to the kinase active site below. Alternatively, by covering the ATP-binding cleft, KaiA may prolong the residence time of ATP, consistent with direct measurements of the dephosphorylation rate of turnover (Xu *et al*, 2003).

### **Stoichiometry of the KaiA–KaiC interaction**

It has been observed that a single KaiA dimer is sufficient to upregulate the phosphorylation of a KaiC hexamer to saturated levels (Hayashi *et al*, 2004a). This suggests that the KaiA dimer either moves from the C-terminal peptide of one subunit to another or that the inherent flexibility of the initial KaiA–KaiC interaction enables the apical side of the tethered KaiA dimer to interact with multiple KaiC subunits within the hexamer.

It is possible that two (Hayashi *et al*, 2004a) or perhaps more KaiA dimers are bound to one KaiC hexamer at the

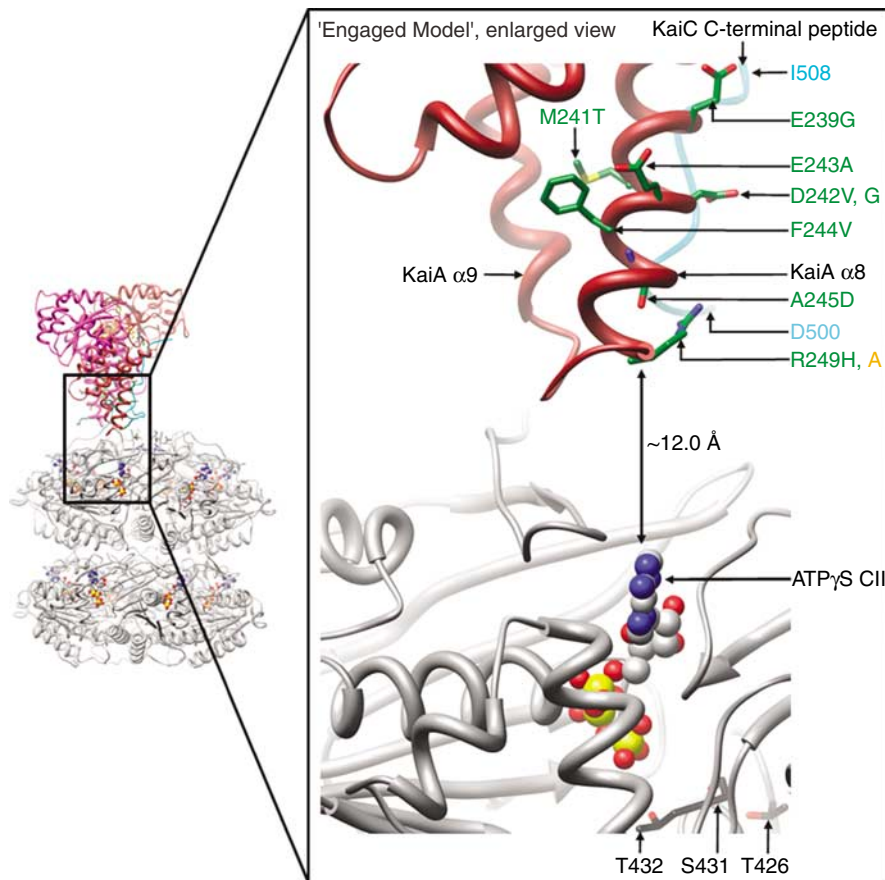


**Figure 9** KaiA–KaiC interactions in the engaged model and mapping of KaiA mutations. Ribbon representation of the engaged model (left) and enlarged view of the boxed region showing the postulated second, functionally important, interaction between KaiA and KaiC (right). Note that the model is rotated with respect to the ribbon-only representation in Figure 8B. Carbon atoms of mutated KaiA residues in the apical region resulting in periods >24 h are shown in stick mode and labeled in dark green. Mutated KaiA residues resulting in periods <24 h are labeled in orange. Carbon atoms of key phosphorylation sites T426, S431, and T432 in KaiC are indicated by arrows. The KaiC C-terminal peptide is colored in cyan and residues at the ends of its visible portion are labeled.

same time. However, this is unlikely to occur *in vivo* because the concentration of KaiC molecules in the cell far exceeds that of KaiA (Kitayama *et al*, 2003; Johnson and Egli, 2004). Under the conditions used for negative-stain EM, we did not observe such a configuration. It is also conceivable that a KaiA dimer might contact two KaiC hexamers simultaneously in order to more efficiently upregulate KaiC's phosphorylation levels. An investigation of circadian formation of clock protein complexes by Kai proteins and SasA in cyanobacteria did not identify heteromultimeric complexes with molecular weights >700 kDa (Kageyama *et al*, 2003) ( $M_r$  KaiA–KaiC 1:2 complex = 773 kDa), and we did not observe this configuration by EM with any appreciable frequency. Therefore, we conclude that a 1:1 stoichiometry of one KaiA dimer to one KaiC hexamer is most likely the biologically relevant form of the complex.

### Conclusions

Integrating insights from electron microscopy and X-ray crystallography with clock behavior as a result of mutations of Kai proteins has enabled us to build a model of the complex between KaiA and KaiC with the apical region of KaiA in proximity to the ATP binding cleft on KaiC. This

model is consistent with all existing structural and functional data and demonstrates for the first time how a KaiA dimer—its role being that of an enhancer of KaiC phosphorylation (or inhibitor of dephosphorylation)—might interact with the KaiC hexamer, the central cog of the cyanobacterial circadian clock. In the model, a helix–loop–helix ( $\alpha 8$ -turn- $\alpha 9$ ) segment from KaiA is in close proximity to the ATP-binding cleft between adjacent KaiC subunits. Mutation of highly conserved residues from the  $\alpha 8$  helix generates phenotypes with periods >>24 h (Ishiura *et al*, 1998; Nishimura *et al*, 2002; Uzumaki *et al*, 2004). The model cannot provide a definitive answer regarding the mechanism of enhancement of KaiC's phosphorylation status by KaiA (i.e. via increase of phosphorylation or reduction of de-phosphorylation). However, it is reasonable to predict that KaiA will alter the binding affinity of ATP through a modulation of conformation and/or electrostatics, thereby facilitating the inter-subunit phosphoryl transfer to residues T426, S431 and T432 (Nishiwaki *et al*, 2004; Pattanayek *et al*, 2004; Xu *et al*, 2004). Since the docking of KaiA to KaiC in this manner would effectively seal the ATP binding site from the outside, it is likely that KaiA's effect is somehow linked to a prolonged residence time of the ATP molecule.

The insights regarding the mode of interaction between KaiA and KaiC gained here also allow us to draw conclusions with respect to the roles of the KaiCI and CII halves, which are obviously the result of a gene duplication (Ishiura *et al*, 1998; Iwasaki *et al*, 1999; Leipe *et al*, 2000), in the generation of circadian rhythm in cyanobacteria. Most importantly, their functions are divergent with the CI hexamer providing a structural platform and the CII hexamer serving as the functional center. Growing evidence can be cited in support of this conclusion. (i) The ATP binding modes between CI and CII differ (Figure 1B) (Pattanayek *et al*, 2004). (ii) The CI half harbors high-affinity and the CII half low-affinity ATP binding sites (Hayashi *et al*, 2004b). (iii) There are no phosphorylation sites in the CI half (Nishiwaki *et al*, 2004; Xu *et al*, 2004). (iv) KaiA binds to a C-terminal peptide fragment from CII but not to the corresponding peptide fragment from CI (Vakonakis and LiWang, 2004). (v) EM and mutational data are consistent with KaiA binding exclusively to the CII half (this work). All of the above shows that the earlier postulates of a binding site for KaiA on KaiC involving CI at the waist region (Taniguchi *et al*, 2001; Vakonakis *et al*, 2004) or the channel (Wang, 2005) are unlikely. Indeed, the lack of phosphorylation sites in CI eliminates the need to evoke an enhancer of phosphorylation status in CI.

The experimental data and modeling efforts presented here improve our understanding of the KaiA–KaiC complex and some of the protein–protein interactions that are key to the generation of the circadian oscillator in cyanobacteria. Much remains to be done in terms of the structural and functional dissection of the whole KaiABC clock system. Similar approaches as those employed here to create a structural model of the KaiA–KaiC complex may furnish useful models of the ternary complex. However, it is clear that high resolution structures of the binary and ternary complexes in combination with more functional studies will be essential for a complete understanding of the biological clock in cyanobacteria.

## Materials and methods

### Expression and purification of wild-type and mutant Kai proteins

The SeKaiA and SeKaiC proteins with (His)<sub>6</sub>-tags were produced in *Escherichia coli* as previously described (Mori *et al*, 2002; Pattanayek *et al*, 2004). His-tagged versions of the ThKaiA and ThKaiC proteins were expressed in *E. coli* and purified by affinity and gel filtration chromatography. ThKaiA and ThKaiC were purified as dimer and monomer, respectively. ThKaiC was hexamerized with AMPPNP following the approach by Hayashi *et al* (2004a). Hexamer formation was assayed using native gel electrophoresis (Figure 4). The construct for the  $\Delta 25CThKaiC$  protein was produced from a plasmid with full-length *ThkaiC* by a restriction digest. The deletion mutant protein was expressed and purified similar to full-length *ThKaiC*. Please see the Supplementary data for details regarding protein expression and purification.

### X-ray crystallography

The crystal structure of P-SeKaiC with PDB-ID code 1U9I (Xu *et al*, 2004) combined with the diffraction data from the SeKaiC crystal (PDB-ID code 1TF7 (Pattanayek *et al*, 2004)) provided the starting point for completing the C-terminal region of the SeKaiC hexamer. The programs TURBO-FRODO (Cambillau and Roussel, 1997) or O (Jones, 2004) were used for map display and model building. All refinements were carried out with the program CNS (Brünger *et al*, 1998) using omit maps to assess the correctness of chain tracing. The final R-work and R-free are 0.23 and 0.29, respectively, using all data to 2.8 Å resolution. The r.m.s. deviations from standard values

for bond lengths and angles are 0.025 Å and 2.1°, respectively. In total, 97% of residues fall into favored regions, 1.9% into generously allowed regions, and 1.1% into disallowed regions. Please see the Supplementary data for details regarding crystallographic procedures.

### Gel electrophoresis

Native PAGE was carried out on a PhastSystem (Pharmacia LKB) using PhastGel Gradient 4–15% gels and PhastGel Native Buffer Strips (Amersham Biosciences). The gels were stained with 0.1% PhastGel Blue R solution in 10% acetic acid and 30% methanol.

### Electron microscopy

Samples were negatively stained with 0.75% uranyl formate. Digital electron micrographs were collected on an FEI Tecnai-12 transmission electron microscope (120 kV, LaB<sub>6</sub> filament) equipment with a Gatan UltraScan 1000 CCD camera using various underfocus levels. The EMAN program Boxer (Ludtke *et al*, 1999) was used for semiautomatic selection of individual particle images from micrographs. The IMAGIC software package (van Heel *et al*, 1996) was used for image classification and angular reconstitution to produce initial three-dimensional reconstructions. The IMAGIC reconstructions were used as starting models for further refinement with the EMAN program Refine. The resolutions of the final reconstructions were assessed with the EMAN program Eotest and the Fourier shell correlation (FSC) 0.5 threshold criterion. Six-fold symmetry (C6) was imposed on the ThKaiC and SeKaiC data sets, and no symmetry was imposed on the ThKaiA–KaiC, SeKaiA–KaiC, and  $\Delta 25CThKaiC + ThKaiA$  data sets. For comparison with the EM data, the KaiA and KaiC crystal structures were converted to 25 Å resolution density maps. Please see the Supplementary data for more details.

### *S. elongatus* strains, KaiC mutagenesis, immunoblotting assay, and in vivo rhythm measurements

The host strain for expression of wt or mutant KaiCs has an in-frame deletion of the endogenous *kaiC* gene (*kaiC*-null) (Xu *et al*, 2003) and the R488A mutation in SeKaiC was generated by site-directed mutagenesis (Xu *et al*, 2004). The construct for expression of the  $\Delta 30CSeKaiC$  protein was obtained by introducing a translational stop codon and removing the 3'-end DNA sequence using PCR. Rhythm measurements using an IPTG-derepressible heterologous promoter were conducted as described in (Xu *et al*, 2003) and immunoblotting was performed as reported previously (Xu *et al*, 2004). Please see the Supplementary data for more details.

### Model building

The SeKaiC (PDB-ID 1TF7, Pattanayek *et al*, 2004) and SeKaiA (PDB-ID 1R8J, Ye *et al*, 2004) crystal structures were fit into the envelope (Figure 8) obtained from the ThKaiA–KaiC EM reconstruction (Figure 5C, bottom row). The SeKaiC crystallographic model was initially translated and rotated into the EM-based density by hand and then iteratively refined with the Chimera FitMap tool (Pettersen *et al*, 2004). Similar procedures were used for optimizing the SeKaiA model in the 'engaged' and 'tethered' orientations. Please see the Supplementary data for details regarding construction and refinement of EM-based models.

### Coordinates

Final coordinates for the crystallographic model of *S. elongatus* KaiC with extended C-termini have been deposited in the Protein Data Bank (PDB ID code 2GBL).

### Supplementary data

Supplementary data are available at *The EMBO Journal* Online.

## Acknowledgements

Support for clock research by the Vanderbilt University Medical Center Intramural Grants Program (Discovery Grant to ME and CHJ) and the National Institutes of Health (R01 GM073845 to ME, R01 GM067152 to CHJ and F32 GM071276 to DRW) is gratefully acknowledged. We would like to thank Dr Satoshi Tabata (Kazusa DNA Research Institute) for providing *T. elongatus* BP-1 genomic DNA, and Susan Opalenik at the Vanderbilt Molecular Genetics Core laboratory for help in subcloning the  $\Delta 25CThKaiC$  deletion mutant.

## References

- Brünger AT, Adams PD, Clore GM, DeLano WL, Gros P, Grosse-Kunstleve RW, Jiang JS, Kuszewski J, Nilges M, Pannu NS, Read RJ, Rice LM, Simonson T, Warren GL (1998) Crystallography and NMR System: a new software suite for macromolecular structure determination. *Acta Crystallogr D* **54**: 905–921
- Cambillau C, Roussel A (1997) *Turbo Frodo, Version OpenGL.1*, Université Aix-Marseille II. France: Marseille
- Dunlap JC, Loros JJ, DeCoursey PJ (2004) *Chronobiology: Biological Timekeeping*. Sunderland, MA: Sinauer
- Garces RG, Wu N, Gillon W, Pai EF (2004) Anabaena circadian clock proteins KaiA and KaiB reveal potential common binding site to their partner KaiC. *EMBO J* **23**: 1688–1698
- Golden SS (2004) Meshing the gears of the cyanobacterial circadian clock. *Proc Natl Acad Sci USA* **101**: 13697–13698
- Hayashi F, Ito H, Fujita M, Iwase R, Uzunaki T, Ishiura M (2004a) Stoichiometric interactions between cyanobacterial clock proteins KaiA and KaiC. *Biochem Biophys Res Comm* **316**: 195–202
- Hayashi F, Itoh N, Uzunaki T, Iwase R, Tsuchiya Y, Yamakawa H, Morishita M, Onai K, Itoh S, Ishiura M (2004b) Roles of two ATPase-motif-containing domains in cyanobacterial circadian clock protein KaiC. *J Biol Chem* **50**: 52331–52337
- Hayashi F, Suzuki H, Iwase R, Uzunaki T, Miyake A, Shen J-R, Imada K, Furukawa Y, Yonekura K, Namba K, Ishiura M (2003) ATP-induced hexameric ring structure of the cyanobacterial circadian clock protein KaiC. *Genes Cells* **8**: 287–296
- Hitomi K, Oyama T, Han S, Arvai AS, Getzoff ED (2005) Tetrameric architecture of the circadian clock protein KaiB: a novel interface for intermolecular interactions and its impact on the circadian rhythm. *J Biol Chem* **280**: 18643–18650
- Ishiura M, Kutsuna S, Aoki S, Iwasaki H, Andersson CR, Tanabe A, Golden SS, Johnson CH, Kondo T (1998) Expression of a gene cluster kaiABC as a circadian feedback process in cyanobacteria. *Science* **281**: 1519–1523
- Iwasaki H, Nishiwaki T, Kitayama Y, Nakajima M, Kondo T (2002) KaiA-stimulated KaiC phosphorylation in circadian timing loops in cyanobacteria. *Proc Natl Acad Sci USA* **99**: 15788–15793
- Iwasaki H, Taniguchi Y, Kondo T, Ishiura M (1999) Physical interactions among circadian clock proteins, KaiA, KaiB and KaiC, in cyanobacteria. *EMBO J* **18**: 1137–1145
- Johnson CH (2004) Precise circadian clocks in prokaryotic cyanobacteria. *Curr Issues Mol Biol* **6**: 103–110
- Johnson CH, Egli M (2004) Visualizing a biological clockwork's cogs. *Nat Struct Mol Biol* **11**: 584–585
- Jones TA (2004) Interactive electron-density map interpretation: from INTER to O. *Acta Crystallogr D* **60**: 2115–2125
- Kageyama H, Kondo T, Iwasaki H (2003) Circadian formation of clock protein complexes by KaiA, KaiB, KaiC, and SasA in cyanobacteria. *J Biol Chem* **278**: 2388–2395
- Kitayama Y, Iwasaki H, Nishiwaki T, Kondo T (2003) KaiB functions as an attenuator of KaiC phosphorylation in the cyanobacterial circadian clock system. *EMBO J* **22**: 1–8
- Leipe DD, Aravind L, Grishin NV, Koonin EV (2000) The bacterial replicative helicase DnaB evolved from a RecA duplication. *Genome Res* **10**: 5–16
- Ludtke SJ, Baldwin PR, Chiu W (1999) EMAN: semiautomated software for high-resolution single-particle reconstructions. *J Struct Biol* **128**: 82–97
- Mori T, Saveliev SV, Xu Y, Stafford WF, Cox MM, Inman RB, Johnson CH (2002) Circadian clock protein KaiC forms ATP-dependent hexameric rings and binds DNA. *Proc Natl Acad Sci USA* **99**: 17203–17208
- Nakahira Y, Katayama M, Miyashita H, Kutsuna S, Iwasaki H, Oyama T, Kondo T (2004) Global gene repression by KaiC as a master process of prokaryotic circadian system. *Proc Natl Acad Sci USA* **101**: 881–885
- Nakajima M, Imai K, Ito H, Nishiwaki T, Murayama Y, Iwasaki H, Oyama T, Kondo T (2005) Reconstitution of circadian oscillation of cyanobacterial KaiC phosphorylation *in vitro*. *Science* **308**: 414–415
- Nishimura H, Nakahira Y, Imai K, Tsuruhara A, Kondo H, Hayashi H, Hirai M, Saito H, Kondo T (2002) Mutations in KaiA, a clock protein, extend the period of circadian rhythm in the cyanobacterium *Synechococcus elongatus* PCC 7942. *Microbiol* **148**: 2903–2909
- Nishiwaki T, Satomi Y, Nakajima M, Lee C, Kiyohara R, Kageyama H, Kitayama Y, Tamamoto M, Yamaguchi A, Hijikata A, Go M, Iwasaki H, Takao T, Kondo T (2004) Role of KaiC phosphorylation in the circadian clock system of *Synechococcus elongatus* PCC 7942. *Proc Natl Acad Sci USA* **101**: 13927–13932
- Pattanayek R, Wang J, Mori T, Xu Y, Johnson CH, Egli M (2004) Visualizing a circadian clock protein: crystal structure of KaiC and functional insights. *Mol Cell* **15**: 375–388
- Taniguchi Y, Yamaguchi A, Hijikata A, Iwasaki H, Kamagata K, Ishiura M, Go M, Kondo T (2001) Two KaiA-binding domains of cyanobacterial circadian clock protein KaiC. *FEBS Lett* **496**: 86–90
- Tomita J, Nakajima M, Kondo T, Iwasaki H (2005) No transcription-translation feedback in circadian rhythm of KaiC phosphorylation. *Science* **307**: 251–254
- Uzunaki T, Fujita M, Nakatsu T, Hayashi F, Shibata H, Itoh N, Kato H, Ishiura M (2004) Crystal structure of the C-terminal clock-oscillator domain of the cyanobacterial KaiA protein. *Nat Struct Mol Biol* **11**: 623–631
- Vakonakis I, LiWang AC (2004) Structure of the C-terminal domain of the clock protein KaiA in complex with a KaiC-derived peptide: implications for KaiC regulation. *Proc Natl Acad Sci USA* **101**: 10925–10930
- Vakonakis I, Sun J, Wu T, Holzenburg A, Golden SS, LiWang AC (2004) NMR structure of the KaiC-interacting C-terminal domain of KaiA, a circadian clock protein: Implications for the KaiA-KaiC Interaction. *Proc Natl Acad Sci USA* **101**: 1479–1484
- Van Heel M, Harauz G, Orlova EV, Schmidt R, Schatz M (1996) A new generation of the IMAGIC image processing system. *J Struct Biol* **116**: 17–24
- Wang J (2005) Recent cyanobacterial Kai protein structures suggest a rotary clock. *Structure* **13**: 735–741
- Williams SB, Vakonakis I, Golden SS, LiWang AC (2002) Structure and function from the circadian clock protein KaiA of *Synechococcus elongatus*: a potential clock input mechanism. *Proc Natl Acad Sci USA* **99**: 15357–15362
- Xu Y, Mori T, Johnson CH (2003) Cyanobacterial circadian clockwork: roles of KaiA, KaiB, and the kaiBC promoter in regulating KaiC. *EMBO J* **22**: 2117–2126
- Xu Y, Mori T, Pattanayek R, Pattanayek S, Egli M, Johnson CH (2004) Identification of key phosphorylation sites in the circadian clock protein KaiC by crystallographic and mutagenetic analyses. *Proc Natl Acad Sci USA* **101**: 13933–13938
- Ye S, Vakonakis I, Ioerger TR, LiWang AC, Sacchettini JC (2004) Crystal structure of circadian clock protein KaiA from *Synechococcus elongatus*. *J Biol Chem* **279**: 20511–20518